JOURNAL OF GUIDANCE, CONTROL, AND DYNAMICS
Vol. 29, No. 1, January–February 2006

Engineering Notes

ENGINEERING NOTES are short manuscripts describing new developments or important results of a preliminary nature. These Notes should not exceed 2500 words (where a figure or table counts as 200 words). Following informal review by the Editors, they may be published within a few months of the date of receipt. Style requirements are the same as for regular contributions (see inside back cover).

Aeroelastic Response of Flapped-Wing Systems Using Robust Estimation Control Methodology

Sungsoo Na*
Korea University, Seoul 136-701, Republic of Korea
Liviu Librescu†
Virginia Polytechnic Institute and State University, Blacksburg, Virginia 24061
Myung-Hyun Kim‡
Pusan National University, Pusan 609-735, Republic of Korea
In-Joo Jeong§
Korea University, Seoul 136-701, Republic of Korea
and
Pier Marzocca¶
Clarkson University, Potsdam, New York 13699-5725

I. Introduction

THE next generation of combat aircraft is likely to operate in more severe environmental conditions than in the past. This implies that, during its operational life, such an aircraft will be exposed to severe conditions including blast, fuel explosion, and sonic boom pulses.[1,2]

As a result, even if its flight is below the flutter speed, the wing structure will be subjected to large oscillations that can yield its failure by fatigue and impair the precision of the mission. All of these facts fully underline the necessity of the implementation of an active control capability enabling one to fulfill two basic objectives: 1) to enhance the subcritical aeroelastic response, in the sense of suppressing the wing oscillations in the shortest possible time; and 2) to expand the flight envelope by postponing the occurrence of flutter instability and so contributing to the increase of the allowable flight speed. During recent years, the great interest in the implementation of aeroelastic control technology was emphasized, among others, in the very comprehensive survey papers by Mukhopadhyay.[3,4] In this Note, using a robust control methodology, the active aeroelastic control of a three-degree-of-freedom (DOF) flapped-wing system exposed to an incompressible flowfield will be investigated.

The controller and the observer are designed based on the mathematical model that considers both measured and estimated states. When the states are not accessible to measurements, they are not considered in the controller and observer design, and their neglect can cause both control and observation spillover. Spillover effects are undesirable and can cause system instability[5] and reduction in performance.[6] As a result, to prevent the occurrence of these undesirable effects, it is required to reduce the observation spillover. To this end, both Kalman filter (KF) and sliding-mode observer (SMO) are implemented, and their relative merits highlighted. The estimator should possess robustness with respect to spillover, model uncertainty, and external excitation. In this sense, sliding-mode observer is introduced to reduce the effect of observation spillover from the states that are not accessible to measurements. The robustness of sliding-mode observer in terms of plant and external excitation uncertainty is not considered here. In this context, the linear-quadratic-Gaussian (LQG) control strategy using SMO will be implemented, and some of its performances will be put into evidence. These will be compared with conventional LQG with Kalman filter. For the purpose of control, in general, not all of the states are available online because of either initial configuration or malfunctions, and the feedback control should be implemented via the estimated states. In this connection, we consider two cases; for one it is possible to measure only the plunging displacement h, whereas in the other case, the measurement of the pitching displacement α is available, only.

II. Configuration of the Three-DOF Flapped-Wing Model

Figure 1 presents the typical wing-flap system that is considered in the present aeroelastic analysis.[7,8] The three degrees of freedom associated with the airfoil appear clearly from Fig. 1. The pitching and plunging displacements are restrained by a pair of springs attached to the elastic axis with spring constants K_α and K_h, respectively. The control flap is located at the trailing edge. A torsional flap spring of constant K_β is also attached at the hinge axis; h denotes the plunge displacement (positive downward), α the pitch angle (measured from the horizontal at the elastic axis of the airfoil, positive nose up), and β is the flap deflection (measured from the axis created by the airfoil at the control flap hinge).

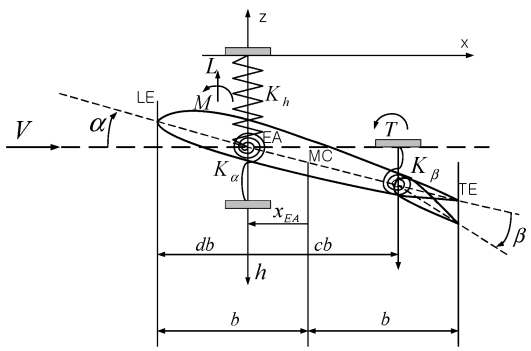

Fig. 1 Typical wing-flap section.

Received 10 December 2004; revision received 26 February 2005; accepted for publication 1 March 2005.

*Associate Professor, Department of Mechanical Engineering. Member AIAA.
†Professor, Department of Engineering Science and Mechanics.
‡Assistant Professor, Department of Naval Architecture and Ocean Engineering.
§Graduate Student, Department of Mechanical Engineering.
¶Assistant Professor, Department of Mechanical and Aeronautical Engineering. Member AIAA.

III. Governing Equation of the Aeroelastic Model

In matrix form the aeroelastic governing equations of the three-DOF flapped-wing system can be written as[9,10]

$$\boldsymbol{M}\ddot{\boldsymbol{Y}}(t) + \boldsymbol{K}\boldsymbol{Y}(t) = -\boldsymbol{L}(t) + \boldsymbol{L}_b f(t) + \boldsymbol{L}_c u(t) \tag{1}$$

where $\boldsymbol{L}(t)$, $\boldsymbol{L}_b f(t)$, and $\boldsymbol{L}_c u(t)$ represent the unsteady aerodynamic loads, blast and control loads, respectively. In Eq. (1), the column vector of plunging/pitching/flapping displacement is defined as

$$\boldsymbol{Y}(t) = [h(t)/b \quad \alpha(t) \quad \beta(t)]^T \tag{2}$$

and

$$\boldsymbol{M} = \begin{bmatrix} bm & S_\alpha & S_\beta \\ bS_\alpha & I_\alpha & I_\beta + bcS_\beta \\ bS_\beta & I_\beta + bcS_\beta & I_\beta \end{bmatrix} \tag{3a}$$

$$\boldsymbol{K} = \begin{bmatrix} bK_h & 0 & 0 \\ 0 & K_\alpha & 0 \\ 0 & 0 & K_\beta \end{bmatrix} \tag{3b}$$

denote the mass and stiffness matrices, respectively.

The second-order aeroelastic governing equation can be cast in the first-order state-space form as

$$\dot{\boldsymbol{x}}(t) = \boldsymbol{A}\boldsymbol{x}(t) + \boldsymbol{B}u(t) + \boldsymbol{G}\boldsymbol{w}(t) \tag{4}$$

Here $\boldsymbol{A}$ is the aerodynamic matrix.[2] The state vector is given by

$$\boldsymbol{x}(t) = [\dot{h}/b \quad \dot{\alpha} \quad \dot{\beta} \quad h/b \quad \alpha \quad \beta \quad B_1 \quad B_2 \quad A_1 \quad A_2]^T \tag{5}$$

where B_1 B_2 A_1 A_2 denote aerodynamic lag states; $u(t)$ is the control input; $\boldsymbol{w}(t)$ is an external disturbance represented by a time-dependent external excitation, such as a blast, sonic boom, or step pressure pulse; $\boldsymbol{G}$ is the disturbance-input matrix, and $\boldsymbol{B}$ is the control input matrix given by

$$\boldsymbol{B} = (1/I_\beta)[(\boldsymbol{M}^{-1}[0\ 0\ 1]^T)^T \quad 0 \quad 0 \quad 0 \quad 0 \quad 0 \quad 0 \quad 0]^T \tag{6}$$

The aerodynamic load vector appearing in Eq. (1) is expressed in terms of its components as

$$\boldsymbol{L}(t) = [L_T(t) \quad M_T(t) \quad T_T(t)]^T$$

$$= [L(t) + L_G(t) \quad M(t) + M_{\mathrm{yG}}(t) \quad T(t) + T_{\mathrm{yG}}(t)]^T \tag{7}$$

where L, M, and T denote, respectively, the aerodynamic lift (positive in the upward direction), the pitching moment about the one-quarter chord of the airfoil (positive nose-down), and the flap torque applied to the flap hinge.

The second terms in expression (7) are caused by the gust. In this respect, for the gust loading we have[11]

$$[L_G(t), M_{\mathrm{yG}}(t), T_{\mathrm{yG}}(t)]$$

$$= \int_0^t [I_{\mathrm{LG}}(t-\sigma), I_{\mathrm{MG}}(t-\sigma), I_{\mathrm{TG}}(t-\sigma)]\frac{w_G}{V}\,\mathrm{d}\sigma \tag{8}$$

where w_G is the gust vertical velocity, while I_{LG}, I_{MG}, and I_{TG} are the related impulse functions. For the present case of the incompressible flow, we have[2,11]

$$I_{\mathrm{LG}} = 4\pi\dot{\psi} \tag{9}$$

$$I_{\mathrm{MG}} = I_{\mathrm{LG}}\left(\tfrac{1}{2} + x_{\mathrm{EA}}/b\right) \tag{10}$$

$$I_{\mathrm{TG}} = 0 \tag{11}$$

where ψ is the Küssner's function, approximated by[11]

$$\psi(\tau) = 1 - 0.5e^{-0.13\tau} - 0.5e^{-\tau} \tag{12}$$

For the expression of aerodynamic loads in the time domain, see Ref. 8.

IV. Design of the Control Law

A. LQG

Within the LQR design of the optimal controller, it is assumed that the entire state vector of the plant to be controlled is available through measurement. However, there are situations of possible sensor failure. In such cases, not all of the states to be controlled are available. As a result, an observer should be constructed in order to estimate the states that are not available, and the feedback control scheme should be implemented via the estimated states. In this sense, assuming that the plant structure and parameters are known completely and accurately, the dynamics of the closed loop estimator are described by

$$\dot{\tilde{\boldsymbol{x}}}(t) = \boldsymbol{A}\tilde{\boldsymbol{x}} + \boldsymbol{B}u(t) + \Lambda[\boldsymbol{y}(t) - \boldsymbol{C}\tilde{\boldsymbol{x}}(t)] \tag{13}$$

$$u(t) = \boldsymbol{K}\tilde{\boldsymbol{x}}(t) \tag{14}$$

where $\tilde{\boldsymbol{x}}$ is the estimate of $\boldsymbol{x}$, while $\boldsymbol{K}$ and Λ denote the control gain matrix and the Kalman-filter gain matrix, respectively. In this connection, one should define the estimation error, that is,

$$\boldsymbol{e}(t) = \tilde{\boldsymbol{x}}(t) - \boldsymbol{x}(t) \tag{15}$$

Furthermore, one needs to consider the effects of internal and external disturbances to the system. To address these issues, an LQG design, which uses noise-corrupted outputs for feedback, is used as a controller. Using LQG method with plant disturbance and sensor noise, the associated equations of motion are represented in state-space form as

$$\dot{\boldsymbol{x}}(t) = \boldsymbol{A}\boldsymbol{x}(t) + \boldsymbol{B}u(t) + \boldsymbol{G}\boldsymbol{w}(t) \tag{16}$$

$$\boldsymbol{y}(t) = \boldsymbol{C}\boldsymbol{x}(t) + \boldsymbol{\pi}(t) \tag{17}$$

The plant disturbance $\boldsymbol{w}(t)$ and sensor noise $\pi(t)$are both assumed to be stationary, zero-mean, Gaussian white noise of intensities Ξ and Θ, respectively, so that their correlation has the form

$$E\left\{\boldsymbol{w}(t_1), \boldsymbol{w}^T(t_2)\right\} = \Xi\delta(t_1 - t_2) \tag{18a}$$

$$E\left\{\boldsymbol{\pi}(t_1), \boldsymbol{\pi}^T(t_2)\right\} = \Theta\delta(t_1 - t_2) \tag{18b}$$

while the processes $w(t)$ and $\pi(t)$ are uncorrelated.

In the preceding equations $E\{\}$ denotes the expected value, δ denotes the Dirac function, and Ξ and Θ are positive definite:

$$\Xi = [I_{10\times 10}] \tag{19a}$$

$$\Theta = [I_{6\times 6}] \tag{19b}$$

B. Sliding-Mode Observer

The controller and the observer are designed based on the mathematical model that considers both the measured and the estimated states only. Because the states that cannot be measured are not considered in the controller and observer design, their neglect can cause both control spillover and observation spillover. For reasons already mentioned, it is required to reduce the observation spillover. To this end, we introduce a sliding-mode observer that reduces the effect of observation spillover from the states that are not measured. In this sense, a sliding-mode observer is designed to provide state estimates. The sliding-mode observer has the form[12]

$$\dot{\tilde{\boldsymbol{x}}} = \boldsymbol{A}\tilde{\boldsymbol{x}} + \boldsymbol{B}u(t) + \Lambda[\boldsymbol{y}(t) - \boldsymbol{C}\tilde{\boldsymbol{x}}] + \Upsilon\boldsymbol{v}(t) \tag{20}$$

where Λ and Υ denote the observer and sliding gain matrices, respectively, and $\boldsymbol{v}(t)$ represents a discontinuous switching component defined as[13]

$$\boldsymbol{v}(t) = \begin{cases} -\Gamma\dfrac{\boldsymbol{T}\boldsymbol{C}\boldsymbol{e}}{\|\boldsymbol{T}\boldsymbol{C}\boldsymbol{e}\|}, & \boldsymbol{e} \neq 0 \\ 0, & \boldsymbol{e} = 0 \end{cases} \tag{21}$$

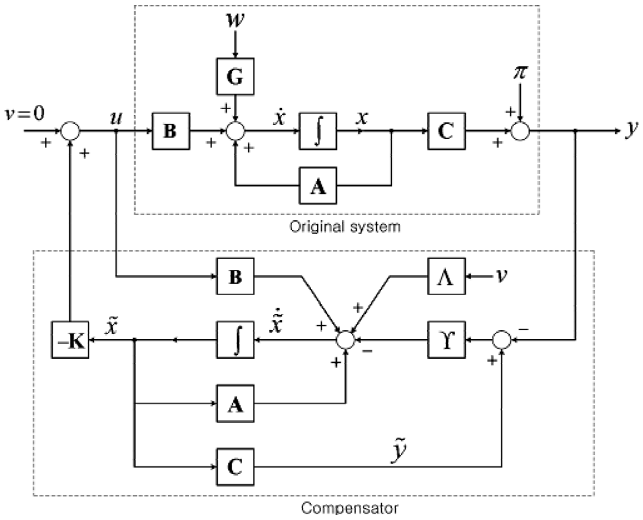

Fig. 2 Block diagram of control system with observer.

In addition, in Eq. (21) T is a positive-definite symmetric matrix, and Γ is a positive scalar function. In agreement with what was shown in Ref. 14, the matrix $\boldsymbol{A}_0 = \boldsymbol{A} - \Lambda \boldsymbol{C}$ satisfies the equation

$$T\boldsymbol{A}_0 + \boldsymbol{A}_0^T T = -\boldsymbol{Q} \tag{22}$$

where $\boldsymbol{Q}$ is a real positive-definite design matrix.

The objective is to induce a sliding motion in the error space

$$S_0 = \{\boldsymbol{e} \in R^n : \boldsymbol{Ce} = 0\} \tag{23}$$

that drives the error $\boldsymbol{e}(t) = \tilde{\boldsymbol{x}} - \boldsymbol{x}$ to zero in finite time despite the presence of the uncertainties in the plant and sensor. The dynamics of estimation error defined as $\dot{\boldsymbol{e}}(t) = \dot{\tilde{\boldsymbol{x}}} - \dot{\boldsymbol{x}}$ becomes

$$\dot{\boldsymbol{e}} = \boldsymbol{A}_0\boldsymbol{e} + \Upsilon\boldsymbol{v} - \boldsymbol{Gw} \tag{24}$$

Note that external excitations appear as disturbances in the error dynamics. With the given form of additional discontinuous input v, the sliding-mode observer can estimate the states of the system. For the stability of observation error dynamics, considering external excitations and using the Lyapunov stability theory, it can be shown that[14]

$$\lim_{t \to \infty} \boldsymbol{e}(t) = 0 \tag{25}$$

which shows that the estimation error is insensitive to disturbance uncertainties.

A block diagram of the LQG control problem using SMO is shown in Fig. 2.

V. Time-Dependent External Pulses

Herein, the case of blast and sonic boom pulses will be considered. As was clearly established, these pressure pulses reach the peak value in such a short time that the structure can be assumed to be loaded instantly. The blast and/or sonic-boom shock pulse can be described by[10]

$$p_y(t) = \begin{cases} P_m[1 - (t/t_p)] & \text{for} \quad 0 < t < rt_p \\ 0 & \text{for} \quad t > rt_p \end{cases} \tag{26}$$

In Eq. (26), P_m denotes the peak reflected pressure in excess of the ambient one; t_p denotes the positive phase duration; r denotes the shock pulse length factor. It can easily be seen that 1) for $r = 1$ the N-shaped pulse degenerates into a triangular pulse, 2) for $r = 2$ a symmetric N-shaped pressure pulse is obtained, whereas 3) for $1 < r < 2$, the N-shaped pulse becomes an asymmetric one.

VI. Results and Discussion

The geometrical and physical characteristics of the three-DOF flapped-wing system to be used in the present numerical simulations are presented in Table 1. The flutter speed for this model is $V_F = 457$ ft/s (139.3 m/s). However, before plunging ourselves into the numerical study, for the sake of validation of the stability methodology used in this Note, the flutter speed, based on the parameters supplied in Refs. 8 and 9, is determined. The critical flutter speed obtained herein via the solution of both the complex eigenvalue problem and from the subcritical aeroelastic response analysis, namely, $V_F = 890$ ft/s (271.3 m/s), coincides with that presented in Refs. 8 and 9. As remarked in Ref. 15, from the mathematical point of view it can be assumed that, instead of moving the flap with a required deflection, an equivalent control hinge moment can be incorporated into the open-loop aeroelastic governing equation (4). This is analytically valid because this external moment acts on the flap hinge and affects only the β DOF. In the presence of external time-dependent excitations, the determination of the time history of the quantities $[\tilde{h}(\equiv h/b), \alpha, \beta]$, at any flight speed lower than the flutter speed, requires the solution of a boundary-value problem.[10] In the absence of the control input, the open-loop aeroelastic response is obtained, whereas in the presence of the control, the closed-loop aeroelastic response is derived.

Figure 3 shows that for the case of the only plunging measurement available as a sensor output the Kalman filter finally produces stable pitching state estimates based on the measurement of plunging displacement only and, consequently, makes the system stable after more than 10 s (Fig. 1 is shown up to 7 s), the obtained data being simulated with the initial conditions $\tilde{h} = 0.01$ and $\alpha = 0.1$ rad and at the flight speed $V_f = 430$ ft/s (131 m/s). Figure 4 reveals that for the case of only pitching measurement available, stable pitching state estimation is achieved in about 3 s through sliding-mode observer with the same initial conditions $\tilde{h} = 0.01$ and $\alpha = 0.1$ rad and $V_f = 430$ ft/s (131 m/s). The same conclusion as in Fig. 4 is reached

Table 1 Geometrical parameters of the wing model

Parameter	Value
b	1 ft (0.3048 m)
x_{EA}	−0.3
K_α	$0.2 \times 100^2 I_\alpha$
K_β	$0.2 \times 300^2 I_\beta$
K_h	0.2×50^2 m
ρ	0.002378 slugs/ft^3 (1.225 kg/m^3)
c	1.0
m	2.6883 slugs/ft (128.7 kg/m)
I_α	1.512 slugs · ft (6.725 kg · m)
I_β	0.0378 slugs · ft (0.168 kg · m)
S_α	0.183894 slugs (2.6838 kg)
S_β	0.030243 slugs (0.4413 kg)

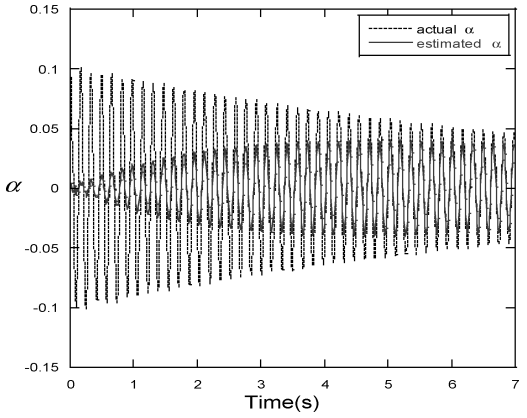

Fig. 3 Performance of estimation using KF with measurable plunging displacement only.

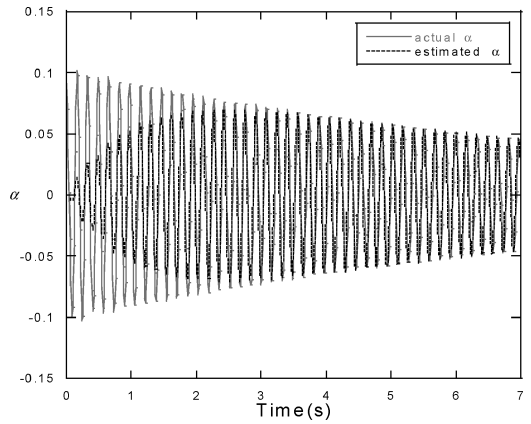

Fig. 4 Performance of estimation using SMO with measurable plunging displacement only.

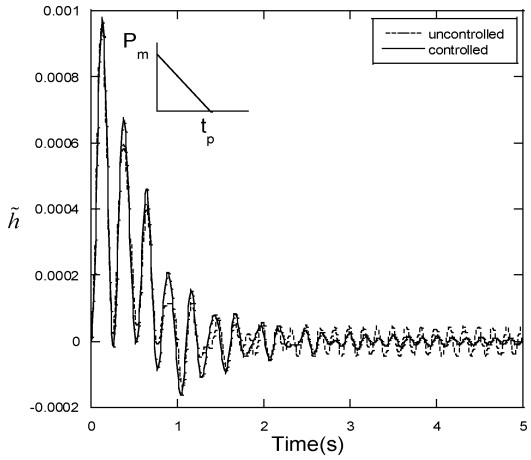

Fig. 5 Uncontrolled/controlled dimensionless plunging time histories of flapped wing subject to a blast.

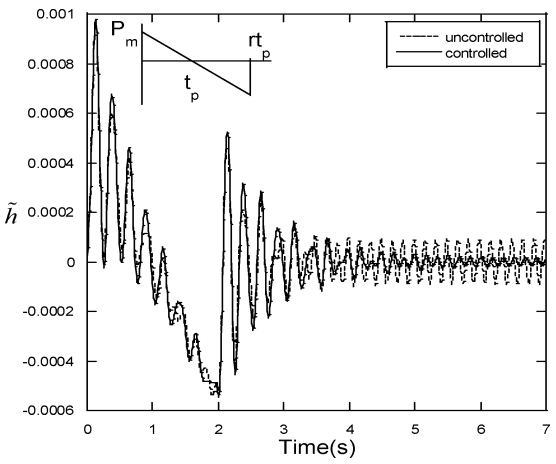

Fig. 6 Uncontrolled/controlled dimensionless plunging time histories of flapped wing to a sonic boom.

in the case of the only pitching measurement through SMO. We should remark that in the same conditions the SMO estimates the state much faster than the KF. As a result, we can conclude that in some extreme situations that involve a sensor failure the SMO is much more preferable to the KF.

Figure 5 displays the uncontrolled/controlled dimensionless plunging aeroelastic time histories of a flapped-wing system operating at $V_f = V_F = 457$ ft/s (139 m/s) subject to a blast pulse [$P_m = 100$ lb/ft (1459.32 N/m)] based on plunging measurement only. From the result, the stable performance of feedback control using sliding-mode observer is experienced. The counterpart of Fig. 5 for the open-closed-loop system exposed to a symmetric sonic boom ($r = 2$), for the same flight speed regime is depicted in Fig. 6. Herein, it is assumed that only the pitching measurement is available. For a speed $V_f < V_F$, it becomes apparent that the amplitude of the response increases with the increase of the flight speed. However, for $V_f = V_F = 457$ ft/s (139 m/s), the response becomes unbounded, implying that the occurrence of the flutter instability is impending. The response to sonic boom pressure pulses involves two regimes: one that corresponds to the forced motion and the other to free motion. The jump appearing in the graph is caused by the discontinuity in the sonic boom pulse occurring at $t_p = 2$s.

VII. Conclusions

Results related to the aeroelastic response and control of three-degree-of-freedom flapped-wing systems operating in an incompressible, subcritical flight speed and exposed to blast/sonic boom loads are presented. The high efficiency of the implemented linear-quadratic-Gaussian control strategy using sliding-mode observer was presented, and the robustness to restricted sensor measurements and external disturbance was revealed. The feedback control system makes use of one measurement, that is of either the plunging or pitching displacement, which is very desirable because of a less computational effort, and also simulates the worst-case scenario, which can happen in the extreme situation of a sensor failure. Moreover, its use can be extended to various flight speed regimes, that is compressible subsonic, transonic, and supersonic ones.

Acknowledgments

Sungsoo Na acknowledges the support by the Basic Research Program of the Korea Science and Engineering Foundation, Grant R01-2002-000-00129-0.

References

[1]Marzocca, P., Librescu, L., and Chiocchia, G., "Aeroelastic Response of a 2-D Lifting Surfaces to Gust and Arbitrary Explosive Loading Signatures," *International Journal of Impact Engineering*, Vol. 25, No. 1, 2001, pp. 41–65.

[2]Librescu, L., Na, S. S., Marzocca, P., Chung, C., and Kwak, M., "Active Aeroelastic Control of 2-D Wing-Flap Systems Operating in an Incompressible Flowfield and Impacted by a Blast Pulse," *Journal of Sound and Vibration*, Vol. 283, Nos. 3–5, 2005, pp. 685–706.

[3]Mukhopadhyay, V., "Flutter Suppression Control Low Design and Testing for the Acting Flexible Wing," *Journal of Aircraft*, Vol. 32, No. 1, 1995, pp. 45–51.

[4]Mukhopadhyay, V., "Historical Perspective on Analysis and Control of Aeroelastic Responses," *Journal of Guidance, Control, and Dynamics*, Vol. 26, No. 5, 2003, pp. 673–684.

[5]Balas, M. J., "Feedback Control of Flexible Systems," *IEEE Transactions on Automatic Control*, Vol. 23, No. 4, 1978, pp. 673–679.

[6]Inman, D. J., "Active Modal Control for Smart Structures," *Philosophical Transanctions: Mathematical, Physical and Engineering Sciences*, 359(1778), 2001, pp. 205–219.

[7]Scanlan, R. H., and Rosenbaum, R., *Introduction to the Study of Aircraft Vibration and Flutter*, Macmillan, 1951 (Dover, 1968).

[8]Edwards, J. W., "Unsteady Aerodynamic Modeling and Active Aeroelastic Control," Stanford Univ., SUDARR 504, Palo Alto, CA, 1977; also NASA CR-148019, 1977.

[9]Olds, S. D., "Modeling and LQR Control of a Two-Dimensional Airfoil," M.S. Thesis, Dept. of Mathematics, Virginia Polytechnic Inst. and State Univ., Blacksburg, VA, April 1997.

[10]York, D. L., "Analysis of Flutter and Flutter Suppression via an Energy Method," M.S. Thesis, Dept. of Aerospace and Ocean Engineering, Virginia Polytechnic Inst. and State Univ., Blacksburg, VA, May 1980.

[11]Dowell, E. H. (ed.), *A Modern Course in Aeroelasticity*, 3rd ed., Kluwer Academic, Dordrecht, The Netherlands, 1995, Chap. 3.

[12]Kim, M. H., and Inman, D. J., "Reduction of Observation Spillover in Vibration Suppression Using a Sliding Mode Observer," *Journal of Vibration and Control*, Vol. 7, No. 7, 2001, pp. 1087–1105.

[13]Edwards, C., and Spurgeon, S., *Sliding Mode Control: Theory and Applications*, Taylor and Francis, 1998, Chap. 6.

[14]Zak, S. H., *Systems and Control*, Oxford Univ. Press, New York, 2003, Chaps. 6 and 8.

[15]Djayapertapa, L., and Allen, C. B., "Numerical Simulation of Active Control of Transonic Flutter," *Proceedings of the 23rd ICAS Congress*, 2002, pp. 411.1–411.10.